CARACTERIZAREA PETROFIZICĂ; PETROGRAFICĂ ŞI MINERALOGICĂ A CALCARENITULUI UTILIZAT PENTRU CONSTRUCŢIA MONUMENTELOR ÎN MAROC
PETROPHYSICAL, PETROGRAPHICAL AND MINERALOGICAL CHARACTERIZATION OF CALCARENITE ROCK USED FOR MONUMENTAL BUILDING IN MOROCCO

MOHAMMED HRAITA[1*] , YOUNES EL RHAFFARI[1], ABDERRAHIM SAMAOUALI[1], YVES GÉRAUD[2], MOHAMED BOUKALOUCH[1]

[1]*Thermodynamics Laboratory, Department of Physics, Faculty of Sciences, Mohammed V University-Agdal, B.P.1014, Rabat, Morocco.*
[2]*Université de Lorraine, Ecole Nationale Supérieure de Géologie, UMR 7359 GéoRessources, Rue du Doyen Marcel Roubault TSA 70605, 54518 Vandoeuvre-lès-Nancy Cedex, France.*

This article consists in studying the petrophysical, petrographical, mineralogical and structural properties of implemented stones. Our study was conducted on one of the stones most commonly used in building monuments of coastal cities in Morocco, particularly in the Rabat-Salé region: the Plio-Quaternary calcarenite. This work is a first phase of a more overall study taking into account the severe conditions to which these building materials were subjected. At this level of advancement, no expertise can be conducted. A good knowledge of various calcarenite stone characteristics allows to better understanding the alteration mechanisms of this material and to consider solutions limiting their progress. So, we have also chosen to work on unaltered samples taken from the original quarry. Experimental analysis performed on sample fragments of unaltered calcarenite rock using the X-ray diffraction (XRD) and the Scanning Electron Microscopy (SEM) observations, allow characterizing the stone both from the mineralogical and the structural point of views. Moreover, the pore size distribution according to pressure-volume analysis has been established by using the mercury intrusion porosimetry method. We will also present petrophysical results concerning the imbibition kinetics, thermal conductivity and permeability for tests performed on specimens taken parallel and perpendicular to the sediment bedding.

1. Introduction

The built heritage represents a cultural reference of utmost importance in all societies. Due to such factors (indifference, lack of financial means…) these heritages were left in an extensive degradation state. Despite from some superficial operations of restoration, no large-scale measure to stop or limit this degradation has been taken. However, only scientific studies can find solutions that are the most appropriate, the least costly, and that lead to the most sustainable results. So, it is necessary to analyze and to understand the mechanisms causing monumental stone alteration before undertaking research on restoration and conservation techniques. Also emphasize the importance of considering the relations between decay factors and highlight how stone properties (mineralogical, hygric and thermal) must be considered as a whole in order to assess and understand the durability of building stones [1].

Generally, the implemented stone alterations are mainly controlled by environmental conditions (rain, cold, sun, wind ...) [1]. These alterations can

also be accentuated by atmospheric pollution, building morphology [2-4] or by the nature of the stone itself (mineralogical composition, porosity structure …) [1,5-7]. Generally, these deteriorations can be grouped into three main categories: the physical alterations (which result from dissociation of the components of the stone without changing the mineralogical composition), the chemical alterations and the biological alterations [7-9]. Indeed, water is the main factor of alteration and degradation phenomena of building materials from historical monuments [10]. These porous building stones can more or less easily adsorb it from the surrounding atmosphere giving rise to a water flow in liquid or vapor state form through the porous network [1]. In these circumstances, the stone is subjected to various alteration types (gel, selective dissolution of minerals, recrystallization, soluble salt transport, favorisation of the biological activity...) [8,9,11,12].

In this context, this work deals with the calcarenite rock, a material widely used by both Romans and Muslims for monumental construction in Morocco. The main objective is to study the

petrophysical, mineralogical and structural properties of this material. Different techniques used are presented and their range of application is discussed. Results are analyzed in order to understand the microscopic and macroscopic observations on the building stone and to identify relations between pore network and water transfer.

2. Material and methods

Calcarenite rock is a coarse bioclastic limestone [6,13]. It corresponds to coastal Plio-Quaternary sandstone outcropping in a more or less continuous manner between Casablanca and Larache [26]. This sedimentary rock, characterized by strong porosity of about 32% [13,14], is composed essentially of calcium carbonate content between 50 and 57%, a low silica content, and iron oxide deposits (about 0,90%) which determine its yellow ocher color [13-15].

Petrophysical measurements are generally carried out on samples extracted from building stone coming from the monuments or the quarry. Samples, studied in this work, were taken from quarry in the Rabat area, which is the origin of the selected rock. A calcarenite block of 12 cm side was used for coring eight identical cylindrical specimens of 33 mm in length and 50 mm in diameter, four specimens were taken in parallel to the sediment bedding (series 1) and four other perpendiculars with this one (series 2) (Fig. 1).
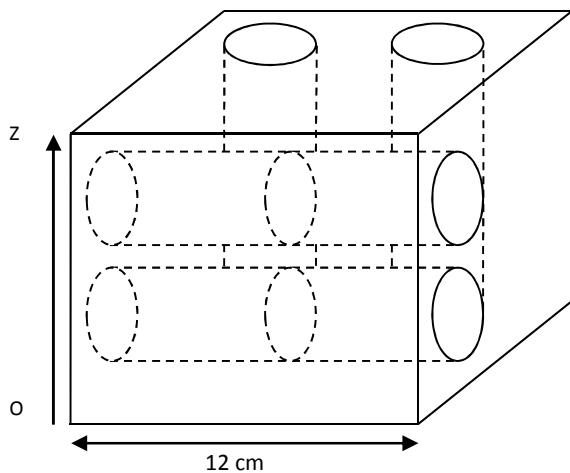
Fig.1 - Coring technique of a calcarenite sample; the axis OZ is perpendicular to the sediment bedding.

2.1. XRD and SEM analysis

The samples were characterized by X-ray diffraction (XRD). The measurements are performed on a granulometry powder of less than two microns in order to have a homogeneous diffractogram, averaging the intensities diffracted by different crystallites. Sample fragments were also observed after a metallization step, by scanning electron microscopy (SEM), coupled to an EDX spectrometer.

2.2. Mercury porosimetry

The total porosity analysis was carried out using mercury intrusion porosimetry techniques. This method relies on the use of the mercury injection. It allows us to determine the pore size distribution according to pressure-volume data. Its principle consists in injecting mercury, with a given pressure, in an initially vacuum enclosure where the sample is degassed beforehand to 2.6 Pa. This method is based on the following relation (Eq. 1), which connects the mercury injection pressure P_{Hg} to the pore access radius R_C.

$$P_{Hg}(MPa) = \frac{7,445}{R_c(\mu m)} \qquad (1)$$

The measurements were performed on a Micromeritics Pore Sizer 9320 porosimeter [26] which can approximately cover pore accesses between 400 and 0.06 µm, or pressure from 0.001 to 207 MPa [5]. The measurement takes place in two steps: the low-pressure measurement (0.001 – 0.150 MPa) and the high pressure measurement (0.150 - 207 MPa) automatically carried out. The uncertainty on the total porosity value is about 4% [14].

2.3. Thermal conductivity scanner

The optical TCS measurement is a stationary method, which consists of measuring the temperature at various points on the sample surface. It is widely used in geothermal and petrophysical studies, particularly as applied to research on cores from deep scientific boreholes [16]. The device used in this technique comprises a mobile carriage, placed just below the platform on which are arranged the test samples. This block has a heat source, on both sides of which are incorporated two sensitive temperature sensors T1 and T2 (Fig. 2).
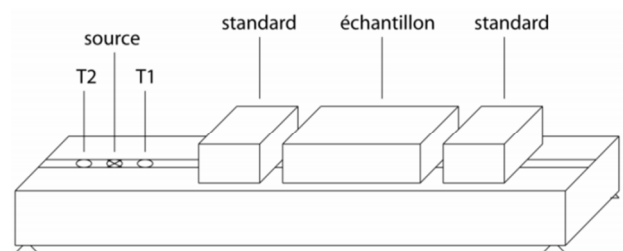
Fig.2 - The device diagram TCS of thermal conductivity measurement; Provision of the standards and the sample during measurement. T1 and T2: temperature sensors.

The heat source and the sensors are aligned parallel to the displacement axis, so that it is possible to determine the thermal conductivity at each point along a line measurement with a millimeter resolution. To make a measurement, the sample is positioned between two identical

standards of known thermal conductivity (Fig. 2). The measurable conductivity ranges between 0,2 and 70 (W/m.K). The merits of optical scanning include minor random errors of about 1,6% [16].

2.4. Tiny Perm II

Tiny Perm II is a device comprising a vacuum cylinder coupled to a pressure transducer enclosure, and a digital control unit. Its principle consists to push air in the specimen along its generatrix and note the value given by the control unit. Tiny Perm II measurement can be cross-referenced to the included calibration curves in order to obtain absolute permeability.

2.5. Imbibition kinetics

The capillary imbibition was carried out by an experimental technique inspired from the protocol test No.II.6 of standard RILEM (1978). The specimens are beforehand oven-dried at 60°C until constant dry weight. They are placed vertically on a rack, then in a tray closed hermetically by a sealing cover that maintains a hygroscopy close to saturation. The water level of about 3 mm is kept constant at the bottom of the tray throughout all experiment duration performed in an air-conditioned room with 25 ° C [17]. The specimen, whose base is in contact with the water film, undergoes a progressive imbibition resulting in an upward extension of the wet zone (the capillary fringe) which results in an increase in its weight. The height of the capillary front (h) and the water mass uptake (Dm) per surface area unit (S) were

then measured as a function of time (in minute) until saturation.

3. Results and discussion

3.1. Mineralogical and petrographical study

It is apparent from the diffractogram (Fig. 3) of a calcarenite sample taken on initial block that the main mineralogical phases constituting the crystal structure of the rock are:

- The silica SiO_2 form of quartz of hexagonal structure (main peak at D_{011} = 3,34 Å) in minor quantity of about 6%;
- The Calcite $CaCO_3$ in majority amount of around 70,97% of rhombohedral structure (main peak at d_{104} = 3,03 Å). This phase is characterized by a rhombohedral crystal system nested closely in the stone matrix.
- The absence of clay minerals in the sample.

The SEM observations (Fig. 4) showed that the microstructure of this material comprises two families of calcite grains. The first family corresponds to the primary angular grains (Fig. 4b) of plurimetric sizes being able to reach a few hundred microns. Their less compact arrangement generates empty spaces (Fig. 4a) inducing an important porosity of relatively elongated form. The second family comprises secondary grains of rhombohedral forms (Fig. 4c, 4d) and micrometric size (between 5 and 50 µm) forming a cement. These sparitic grains are precipitated between the primary grains and decrease the macropore size
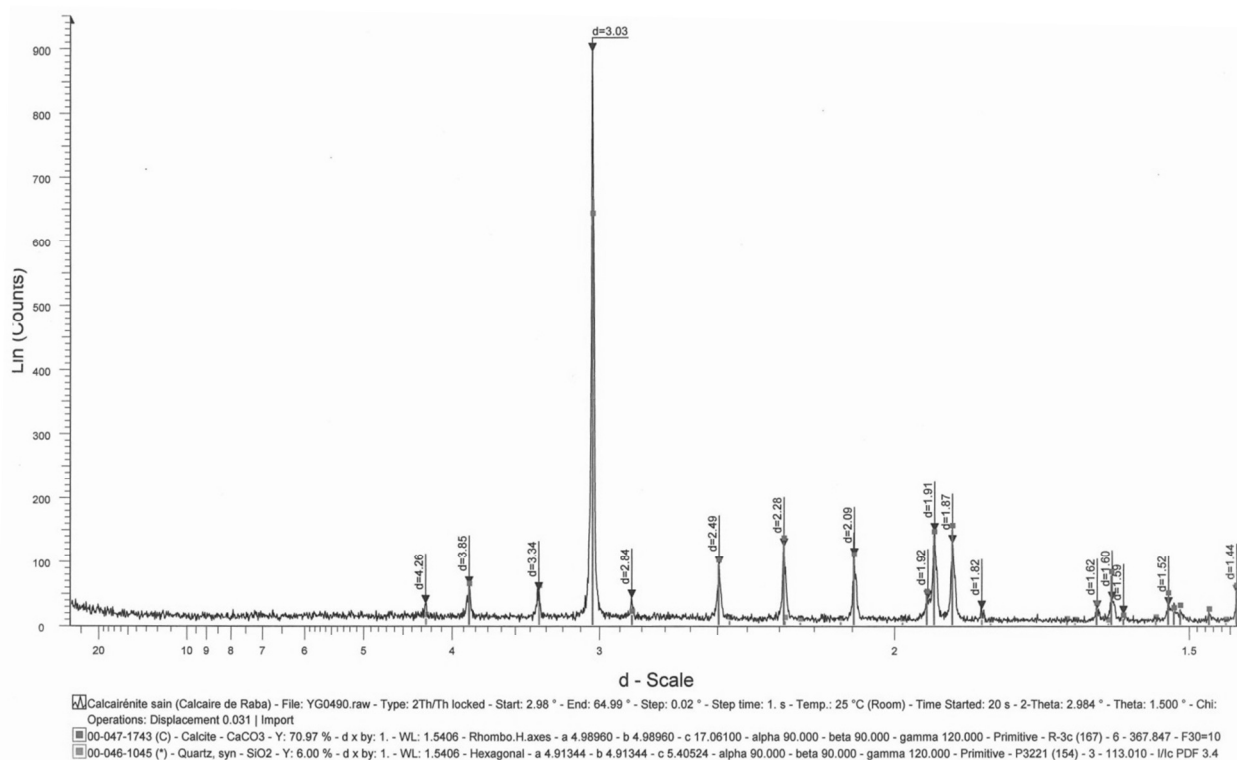
Fig.3 - Diffractogram obtained from a powder for unaltered calcarenite stone.
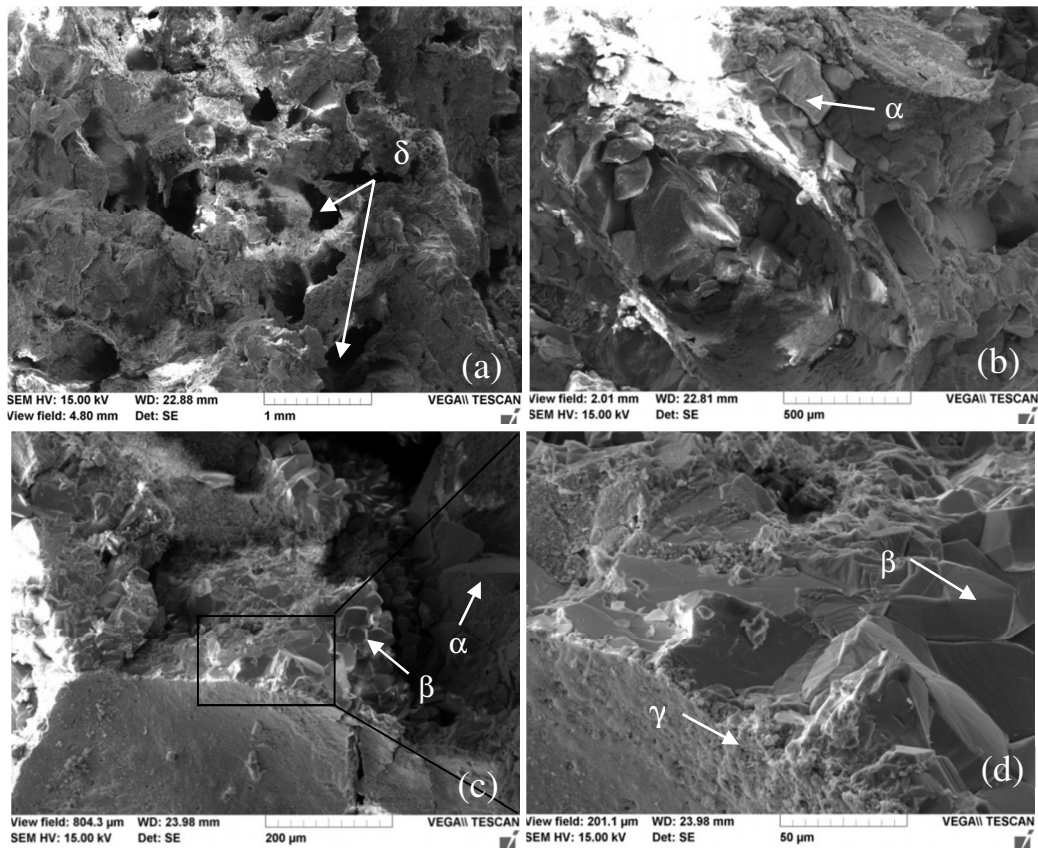
Fig.4 - Images taken using an SEM on calcarenite rock fragments at different scales: (a) : x20 ; (b) : x40 ; (c) : x100 ; (d) : x400.

Table 1

Results of mercury porosimetry measurements

	EX1	EX2	EZ1	EZ2
Total porosity N_{Hg} (%)	29.61	24.48	27.9	22.44
Trapped porosity N_{HgP} (%)	4.12	2.14	3.45	3.63
Free porosity N_{HgL} (%)	25.49	22.34	24.45	18.81
Macroporosity (%)	23.05	19.73	22.62	17.09
Microporosity (%)	6.56	4.75	5.28	5.35
Apparent density g/cm^3	2.67	2.63	2.8	2.45
Threshold access diameter Da (µm)	156.79	156.86	156.69	156.67
Average pore diameter (µm)	3.078	2.404	1.985	1.530
Specific surface (m^2/g)	0.2047	0.2054	0.278	0.309
Dispersion coefficient (Cd)	1.8	1.45	1.3	1.74

promoting their trapping. One also observes the presence of a micritic calcite coating (Fig. 4d), which comprises very fine crystals (lower to 4µm). These aggregates form a thick layer of about 20 µm, which can clog the secondary grains constituting the microporosity of the material and also promoting the trapping of macropores. Thus, the calcarenite rock structure can be compared to an assembly of micritic grains, and detritus elements by sparitic cement. The inhomogeneous stacking of these grains promotes inter-granular spaces presenting irregularities of size and form and communicating via wider or less wide connections.

3.2. Mercury porosimetry

The analysis by mercury porosimetry was performed on four samples having a volume of

1 cm^3, taken in two different directions EX and EZ in order to represent the entire block. EX1 and EX2 are two samples selected according to the bedding plane and taken in the same area as specimens of series 1, EZ1 and EZ2 are two samples taken perpendicularly from this plane, in the same area as that of the test series 2.

Results presented in Table 1 shows that the total porosity of the samples varies between 22.44 and 29.61%. This rather strong porosity, typical of the calcarenite rocks, corresponds to a relatively weak apparent density ranging between 2.45 and 2.8 g/cm^3. These values demonstrate an important heterogeneity of the studied material. The measurement, low pressure, inform about the macroporosity value, i.e. porous volume accessible by the pore access radiuses ranging

between 7.5 and 100 µm. Indeed, the lower limit of the macropore radiuses, according to [18] is 7.5 µm, which corresponds to a pore access diameter of 15 µm and a pressure of 1 bar. According to our results (Tab. 1), the porosity of the calcarenite stone is thus essentially of macroporous type. The presence of angular grains of large sizes in the solid matrix seems to be the cause of this macroporosity. Mercury porosimetry thus allows quantifying the observations made by SEM.

This technique also allows measuring the specific surface area corresponding to the sum of the surfaces developed by the particles forming the skeleton of the porous medium (and thus the surface of the pore walls) for a unit mass of the porous material. This surface is capable to fix molecules by adsorption and varies mainly according to the pore size and the importance of the clay fraction. It's on the level of this surface that the heat exchanges between rock and fluid are carried out. From the practical point of view, the determination of this surface amounts to calculating the delimited air above the mercury injection curve. The specific surface area determined by this method cannot be considered as an absolute value; it is generally less than the specific surface area measured by the BET method. Its value (Tab. 1), inversely proportional to the average pore diameter, is relatively weak (about 0,2 m²/g for EX1 and EX2 and 0.3 m²/g for EZ1 and EZ2). For comparison, the specific surface area of montmorillonite (a swelling clay) is about 80 m²/g, that of biotite (black mica) is about 4.5 m²/g and that of glass powder is of 0.3 − 0.4 m²/g [19], that of the Fontainebleau Sandstone is less than 0.02 m²/g and about 1 m²/g for the micrite [20]. The low value of the specific surface area developed by this material is easily explained by the absence of minerals of high specific surface area such as the case of the clays.
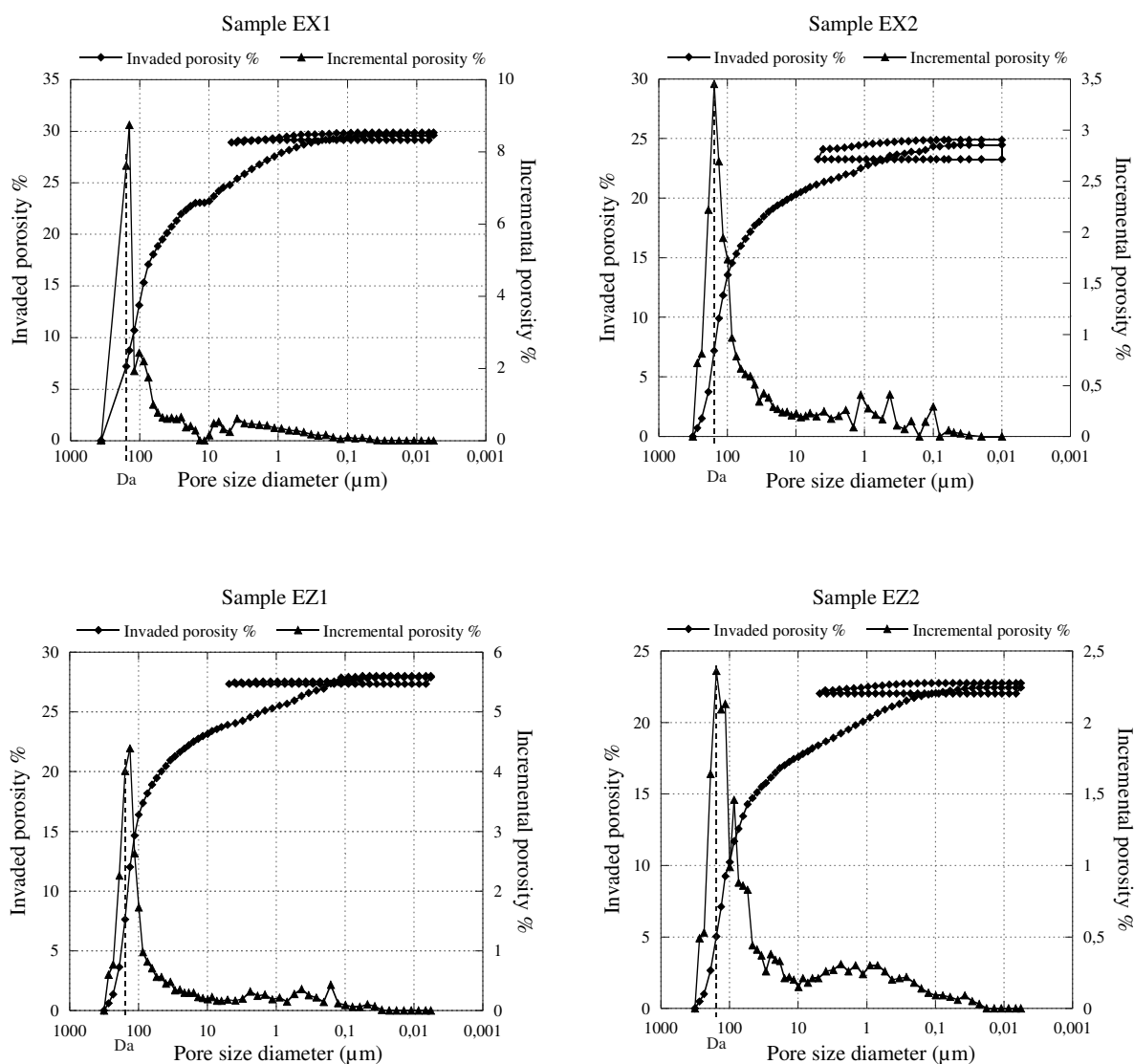
Fig.5 - Mercury porosimetry curves of calcarenite samples EX1, EX2, EZ1 and EZ2; Da is the threshold pore access diameter.

The spread porosimetric spectrum is measured by a dispersion coefficient, Cd, calculated based on a report of injection pressures (Eq. 2) [21-23]:

$$Cd = \frac{P_{80} - P_{20}}{P_{50}} = \frac{R_{20} - R_{80}}{R_{50}} \quad (2)$$

where P_{80}, P_{50} and P_{20} are the mercury injection pressures corresponding to the invasion of 80, 50 and 20% of the porous medium. This can be brought back to the report of the pore access radiuses R_{80}, R_{50} and R_{20} correspondents. The value of the dispersion coefficient Cd differs from one sample to another. It is greater than unity, indicating that pore accesses are moderately dispersed and the distribution is spread [5]. We thus have either a unimodal network of spread distribution, or a strict multimodal network or of broad distribution. This distribution corresponds to porous media where dimensional heterogeneities are considered non-random, and the spatial arrangement of pores leads to porous media compartmented in fields of pores with a given size [23].

According to the mercury injection curves (Fig. 5), the pore volume distribution is in general unimodal, characterized by only one dominant pore family which translates into a single inflection point on the injection curve. Consequently, it is possible to determine graphically the threshold pore access diameter Da: it is the largest diameter giving access to the maximum of porous volume. This one appears on the first injection curve like the diameter corresponding to the inflection point of the curve [17,20] (Fig. 5). Its value is almost identical for the four samples and is approximately 156,7 microns (Tab. 1). Another measurable data on mercury injection curves is the trapped porosity NHgP. The values obtained (Tab. 1) show how the difference in size between the cavities and their accesses is much less important in this material. In other words, the low value of trapped porosity

obtained is easily explained by the less strong contrasts existing between the radiuses of cavities and radiuses of constrictions. Indeed, almost all of the volume of mercury introduced remains free during the imbibition: for EX1 for example, NHgP is 4,12% for a total porosity NHg of 29,61%, i.e. that NHgP constitutes 13,91% of the total porosity. This means that the pore network inside the stone is much less favorable to the mercury trapping.

3.3. Thermal conductivity

The building stones are generally the diphasic porous media, made up of a solid phase saturated by only one motionless fluid phase, as it happens by the air. The heat transfer within these heterogeneous media microscopically, can be linked at the macroscopic scale to that of a fictitious continuous medium. The thermal properties of the latter therefore are controlled primarily by the nature and phase distribution which constitute it (mineral composition and texture of the rock) [16]. Indeed, the thermal conductivity (λ) values determined by TCS on dry samples are between 0.972 and 1.1 W/(m.K) for the profiles carried out along the cores generatrix, and between 1.258 and 1.357 W/(m.K) for profiles carried out according to the diameters (Tab. 2). These variations are indicative of an initial heterogeneity of material. Generally, λ is an anisotropic property, but for many rocks the effects of anisotropy are minor compared to the uncertainty introduced by variations in mineral composition [16]. The thermal conductivity of these samples, saturated with water for 24 hours, does not seem to evolve significantly, it varies between 1.328 and 2.141 W/(m.K) according to the generatix, and between 1.699 and 1.804 W/(m.K) according to the diameters (Tab. 3). These results show an increase in the thermal conductivity as a function of water content [16]. In fact, the pore space initially containing air is filled with water having a higher thermal conductivity.

Table 2

Results of thermal conductivity measurements performed on cores in the dry state

	Carrots parallel to the sediment bedding (series 1)				Carrots perpendicular to the sediment bedding (series 2)			
	EP1	EP2	EP3	EP4	EH1	EH2	EH3	EH4
λ- diameter	1.327	1.258	1.345	1.357	1.277	1.342	1.328	1.321
λ- generatrix	1.060	1.043	0.985	0.975	1.100	1.016	0.972	0.982
λ- average	1.194	1.150	1.165	1.166	1.188	1.179	1.150	1.151

Table 3

Results of thermal conductivity measurements performed on samples saturated with water for 24 hours

	Carrots parallel to the sediment bedding (series 1)				Carrots perpendicular to the sediment bedding (series 2)			
	EP1	EP2	EP3	EP4	EH1	EH2	EH3	EH4
λ- diameter	1.699	1.686	1.789	1.804	1.732	1.692	1.793	1.726
λ- generatrix	2.141	1.415	1.356	1.421	1.398	1.328	1.444	1.422
λ- average	1.920	1.550	1.573	1.612	1.565	1.510	1.618	1.574

We can conclude that the thermal conductivities of various samples in the dry state are of the same order of magnitude and are independent of the orientation. Fluctuations obtained in the conductivity values are likely due to the surface state of the material as well as systematic errors of measurements. The material then seems to present a certain isotropy with respect to thermal conductivity. A similar interpretation can be attributed to material saturated with water for 24 hours.

3.4. Permeability

The permeability measurements were carried out on specimens that were parallel (series 1) or perpendicular (series 2) to the stone bedding. For each sample, the value considered for the permeability is the average of the values obtained on each side. These values (Tab. 4) are particularly important and show that the calcarenite stone has a great aptitude for the fluids transfer. This is usually due to the rather high porosity of this material. In addition, the rock permeability also depends on its intrinsic textural properties such as pore size, tortuosity and porous network connectivity [24]. Indeed, [17] showed that the permeability increases with increasing threshold pore diameter but without linear relation between these two parameters, this because of graphical determination mode of threshold diameter and singularity of threshold diameter giving access to a variable percentage of porosity. For example, if we compare the white tuffeau and the Sebastopol stone (Tab. 5), which have a rather strong and similar total porosities, while their threshold

diameter are very different, the permeability increases in the direction of an important macroporosity [7]. This is also observed for limestones of Lerouville and Chassignelle and also for limestones of Vassens and Méry (Tab. 5). This difference confirms that the permeability is more correlated to the threshold pore access diameter and to the macroporosity proportion that to the simple total porosity value [23]. However, the difference of the permeability between limestones of Sireuil and of Mériel (Tab. 5) shows that it is necessary to take into account other parameters other than total porosity and the threshold pore access diameter. For example, sandstone of Vosgien and of Meules are characterized by similar total porosities and threshold diameter, yet have very contrasting permeabilities. This is due to the difference in the clay particle size which are more or less easily mobilized to block some pores and thus decrease the porous network connectivity [5].

We can conclude that the high permeability of the calcarenite stone (Tab. 4) can be explained by the absence of argillaceous grains and large total porosity values, of macroporosity and of the threshold pore access diameter in this material (Tab. 1). We also note that the average permeability values obtained (Tab. 4) are of the same order of magnitude in directions both parallel and perpendicular to the bedding plane. The dispersion of values is mainly due to the heterogeneity of material. Taking into account the different permeability values and its averages (Tab. 4), it seems then that the material in the healthy state has a certain isotropic with respect to permeability.

Table 4

Results of permeability measurements performed on two series of specimens

	Carrots parallel to the sediment bedding (series 1)				Carrots perpendicular to the sediment bedding (series 2)			
	EP1	EP2	EP3	EP4	EH1	EH2	EH3	EH4
Permeability (Darcy)	2.027	2.291	5.014	7.470	5.785	5.341	6.731	4.201
Average (Darcy)	4.200				5.515			

Table 5

Water permeability of some sedimentary rocks [7]

Appellation	Geological Stage (provenance)	Total porosity (%)	Threshold pore diameter (µm)	Permeability (mD)
Lerouville	Rauracien (Meuse)	11	40 et 0.5	170-190
Chassignelle	Bathonien (Yonne)	12	0.25	0.18
Vosgien sandstone	Buntsandstein Moy. (Bas-Rhin)	18	6 et 0.05	0.3-2
Meules sandstone	Buntsandstein Sup. (Haut-Rhin)	23	5	90-120
Sireuil	Cénomanien (Charentes)	35	11 et 0.3	550-750
Mériel	Lutétien Moy. (Val d'Oise)	36	16 et 0.15	75-310
Savonnière	Portlandien Inf. (Meuse)	37	7 et 0.1	60-100
Vassens	Lutétien Inf. (Aisne)	40	14 et 0.13	970-1710
Méry	Lutétien Sup. (Val d'Oise)	41	7 et 0.1	120
Sebastopol stone	Lutétien Moy. (Oise)	42	20	1400
white tuff	Turonien Moy. (Maine-et-Loire)	48	5	100

3.5. Capillary imbibition

During imbibition experiments, measurements of the height of the capillary fringe were difficult for both sets of specimens because the fringe was not very visible, samples were wet irregularly. This makes it difficult to estimate the time put for wetting the whole core. The representative lines of the curve of the capillary fringe are thus not very precise.

Imbibition capillary curves (Fig. 6) show that the more porosity is important (Tab. 6), the higher the imbibition speed. These curves also show the presence of two types of porous networks (unimodal and bimodal), which explains the macroscopic heterogeneity of the material studied. The presence of a bimodal network in cores EP1, EP2, EH2 and EH4 shows a microscopic heterogeneity in this material. Samples EP3, EP4, EH1 and EH3 are characterized by a unimodal network and rather high water porosity compared to other cores (Tab. 6). This network type is translated on the mass uptake curves by a single

break of slope that corresponds to the arrival of the wet fringe at the top of the specimen. Between the two linear portions, there exist an intermediate area of curved shape which results from the superposition of the imbibition phenomenon and that of the air diffusion in water [5]. The shape of the capillary imbibition curves can be explained by the existence of a predominant pore family, well interconnected and evenly distributed in the sample [5,25].

The second bimodal network in cores EP1, EP2, EH2 and EH4, is reflected in the capillary imbibition curves by one (or more) break of slope obtained between the straight characterized by the A_1 slope and the straight of weaker slope A_2. This is explained by the coexistence within the sample, of two pore family: one is well connected and saturated firstly and another less well connected whose filling is more slowly carried out [5,25]. The multiplication of slope break indicates an increasing heterogeneity of a porous network freely interconnected. The cores EH2 and EH4 have bedding planes oriented perpendicularly to
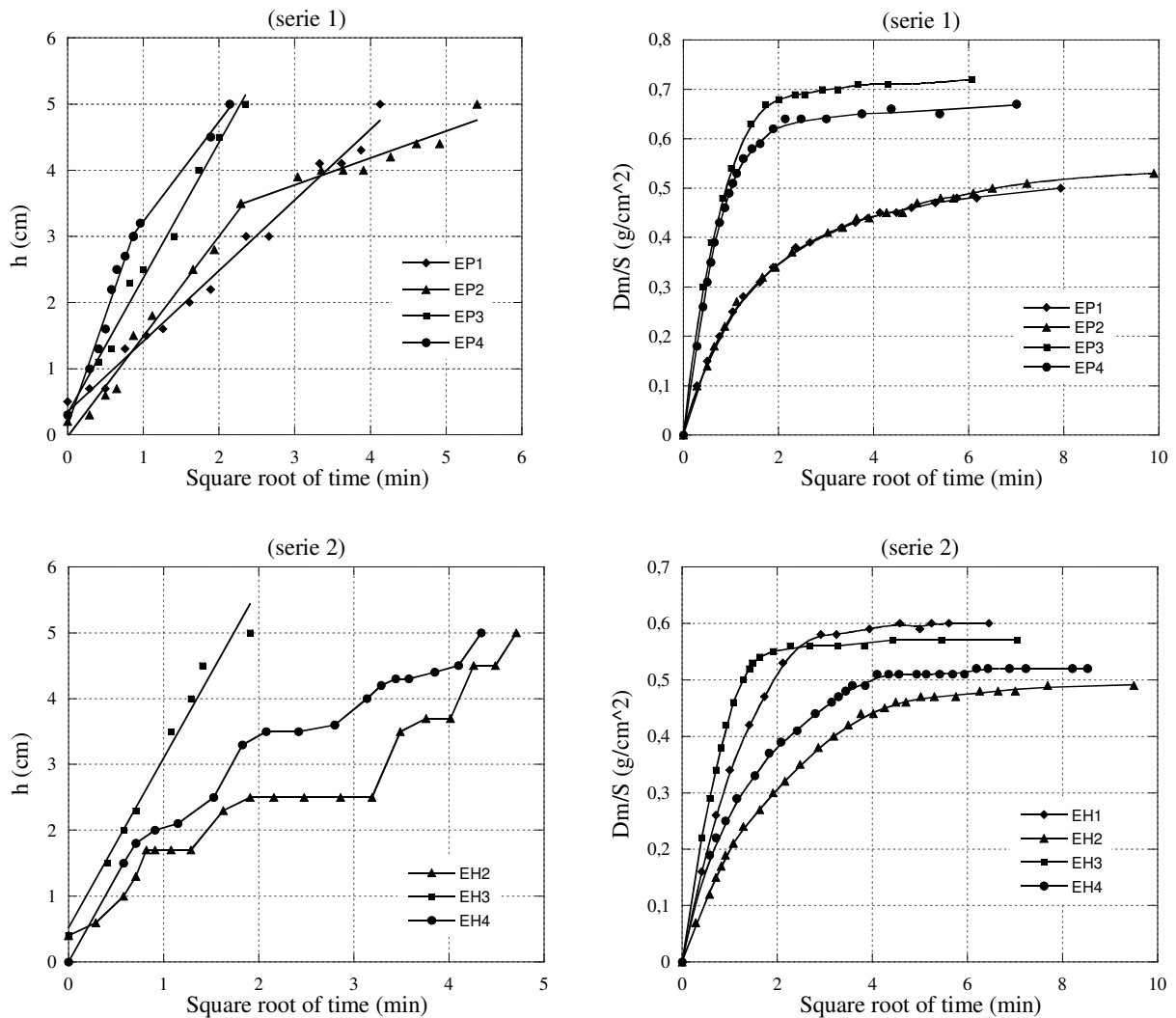
Fig.6 - Curves of the capillary imbibition kinetics performed on the two series of specimens.

Table 6

Water porosity for 24 hours of two series of specimens

	Carrots parallel to the sediment bedding (series 1)				Carrots perpendicular to the sediment bedding (series 2)			
	EP1	EP2	EP3	EP4	EH1	EH2	EH3	EH4
Water porosity (24h)	15.98	16.38	18.27	18.86	19.35	16.31	19.29	17.16

the direction of the imbibition curves; one observes thus curves in staircase marking of the local variations of the imbibition kinetics [20]. If one compares the water mass uptake curve and those of capillary fringe migration, one notices that the capillary fringe arrives at the top of the sample approximately at the second slope break of the mass uptake curve. That is explained by a heterogeneous distribution of two pore family at the level of the specimen [5].

Generally the results of capillary imbibition kinetics are consistent with those of mercury porosimetry and particularly with those of the dispersion coefficient Cd.

The difference between the water porosity and mercury porosity can be explained by:

- The specimens are not degassed beforehand at the time of the water porosimetry;
- 24 hours is not sufficient to fully saturate the porous network of specimens;
- In mercury porosimetry technique, the sample has a limited volume that can be included between 1,5 and 11 cm^3, which poses the problem of its representativeness with respect to the rock [5].

4. Conclusion

We presented in this work the results from the study of the petrophysical, mineralogical and structural properties of unaltered calcarenite rock. Powder X-ray diffraction shows the presence of two major crystalline phases forming the rock structure: calcite and quartz. The SEM observations shows a microstructure characterized by inter- and intra-granular spaces with irregularities in size and shape and communicating by connections more or less wide, which explains the high value of the measured permeability. The less compact arrangement of the grains generates empty spaces inducing an important porosity in the material. The latter, relatively elongated, is located mainly between the primary grains and can be sealed by secondary precipitation. The mercury injection curves and those of the imbibition kinetics show that the calcarenite having high total porosity and low trapped porosity is a macroporous rock, characterized by the coexistence of two pore family: macroporous and microporous. The first family is dominant, well connected and saturated firstly, the second is less well connected and is filled more slowly. Other results highlight the initial isotropy of this material according to the bedding

orientation with respect to thermal conductivity and permeability.

We plan, in perspective, to approach the alteration study of the calcarenite rock by salts precipitation. This study will relate to the same samples of two series and will entail carrying out imbibition-drying cycles with different salt solutions, and thus follow the evolution of different rock properties in order to understand the impact of salt precipitation on its deterioration.

REFERENCES

1. D. Benavente, G. Cultrone and M. Gómez-Heras, The combined influence of mineralogical, hygric and thermal properties on the durability of porous building stones, Eur. J. Mineral, 2008, **20**, 673.
2. L. Leysen, E. Roekens and R. Van Grieken, Air-pollution induced chemical decay of a sandy-limestone cathedral in Belgium, The Science of the Total Environment, 1989, **78**, 263.
3. F. Zezza, Marine spray and polluted atmosphere as factors of damage to monuments in the Mediterranean coastal environment. Eur, Cultural Heritage Newsletter Res, 1993, **7**, 49.
4. V. Fassina, A survey of air-pollution and deterioration of stonework in Venice, Atmospheric Environment, 1978, **12**, 2205.
5. C. Thomachot, PhD thesis, Modifications des propriétés pétrophysiques de grès soumis au gel ou recouverts «d'encroûtements noirs vernissés», Louis Pasteur University of Strasbourg, France, 2002.
6. N. Zaouia, M. EL wartiti and B. Baghdad, Superficial alteration and soluble salts in the calcarenite weathering. Case study of almohade monument in Rabat: Morocco. Environ. Geol., 2005, **48**, 742.
7. K. Beck, PhD thesis, Etude des propriétés hydriques et des mécanismes d'altération de pierres calcaires à forte porosité, University of Orléans, Paris, France, 2006.
8. S. Papida, W. Murphy and E. May, Enhancement of physical weathering of building stones by microbial populations, International Biodeterioration and Biodegradation, 2000, **46**, 305.
9. C. Gaylarde, M. Ribas Silva and Th. Warscheid, Microbial impact on building materials: an overview, Materials and Structures, 2003, **36**, 342.
10. K. Beck, M. Al-Mukhtara, O. Rozenbaum and M. Rautureau, Characterization, water transfer properties and deterioration in tu&eau: building material in the Loire valley France, Building and Environment, 2003, **38**, 1151.
11. M. Angeli, D. Benavente, J.P. Bigas, B. Menéndez, R. Hébert and C. David, Modification of the porous network by salt crystallization in experimentally weathered sedimentary stones, Materials and Structures, 2007, DOI 10.1617/s11527-007-9308-z.

12. G.W. Scherer, Stress from crystallization of salt, Cement and Concrete Research, 2004, **34**, 1613.

13. H. Azouaoui, N. El Hatimi and N. El Yamine, Plio-Quaternary formations of the Casablanca area (Morocco): sedimentological and geotechnical aspects, Bull Eng Geol Environ, 2000, **59**, 59.

14. A. Samaouali, L. Laânab, M. Boukalouch and Y. Géraud, Porosity and mineralogy evolution during the decay process involved in the Chellah monument stones, Environ Earth Sci, 2010, 59, 1171-1181. DOI 10.1007/s12665-009-0106-5.

15. A. Samaouali, L. Laânab, Y. Geraud, A. Nounah and M. Boukalouch, Experimental study of chemical deterioration of Chellah monument stones, Phys. Chem. News 2008, **44**, 103.

16. Y.A. Popov, D. Pribnow, J.H. Sass, C.F. Williams and H. Burkhardt, Characterization of rock thermal conductivity by high-resolution optical scanning, Geothermics, 1999, **28**, 253.

17. J.D. Mertz, PhD thesis, Structures de porosité et propriétés de transport dans les grès, Louis Pasteur University of Strasbourg, France, 1991, 149 pp.

18. I. Goni, J. P. Ragot, and A. Sima, Méthode d'étude du champ microfissural des minéraux et des roches et possibilité d'application en géologie, Bull BRGM (2º série) section II, 1968, **4,** 51.

19. J. Fripiat, J. Chaussidon and A. Jelli, Chimie physique des phénomènes de surface, Edition Masson, Paris, 1971, 387 p.

20. B. Rousset Tournier, PhD thesis, Transferts par capillarité et évaporation dans des roches : rôles des structures poreuses, Louis Pasteur University of Strasbourg, France, 2001, 196 p.

21. N.C. Wardlaw, M. Mckellar and Y. Li, Pore and throat size distributions determined by mercury porosimetry and by direct observation, Carbonates and Evaporites, 1988, **3**, 1.

22. Y. Géraud, PhD thesis, Déformation thermomécanique et porosité des roches granitiques. Evolution des espaces poreux, University of Provence (Aix-Marseille I), 1991, **329** pp.

23. J.M. Rémy, PhD thesis, Influence de la structure du milieu poreux carbonaté sur les transferts d'eau et les changements de phase eau-glace. Application à la durabilité au gel de roches calcaires de Lorraine, Polytechnic National Institute of Lorraine, 1993.

24. Y. Guégen, V. Palciauskas, Introduction à la physique des roches. Éd. Hermann, 1992, 299 pp.

25. A. Chabas, PhD thesis, Rôle de l'environnement atmosphérique marin dans la dégradation des marbres et du granite de Délos (Cyclades - Grèce), University of Paris XII - Val de Marne, 1997.

26. Y. El Rhaffari, M. Hraita , A. Samaouali, M. Boukalouch and Y. Géraud, Thermal and petrophysical characteristics of calcarenite rocks used in the construction of monuments of Rabat, Romanian Journal of Materials 2014, **44**(2), 153.

****

MANIFESTĂRI ŞTIINŢIFICE / SCIENTIFIC EVENTS

ICEMA 2015 : XIII International Conference on Engineering Materials and Applications

Istanbul, Turkey, January 26 - 27, 2015

Conference Objectives

The **ICEMA 2015: XIII International Conference on Engineering Materials and Applications** aims to bring together leading academic scientists, researchers and research scholars to exchange and share their experiences and research results about all aspects of Engineering Materials and Applications. It also provides the premier interdisciplinary and multidisciplinary forum for researchers, practitioners and educators to present and discuss the most recent innovations, trends, and concerns, practical challenges encountered and the solutions adopted in the field of Engineering Materials and Applications.

Contact : http://www.waset.org/topic/Materials-Science-and-Engineering/2015/01/istanbul

****